# Multilayer Hybrid in Circular Waveguide

EARL T. HARKLESS AND DOUGLAS N. ZUCKERMAN, MEMBER, IEEE

*Abstract*—**A dielectric sheet across a waveguide will partially transmit and partially reflect propagating waves. Such a sheet placed at 45° across the right angle intersection of two waveguides can create a hybrid junction. The use of several dielectric layers reduces mode conversion and also broad-bands the performance. It is shown here how to choose the thickness and permittivity of the layers to yield nearly constant power division over the 40- to 110-GHz range and at the same time minimize conversion of energy to other modes. Ray-optics analysis is used in this design procedure. Experimental results are presented which confirm the analysis. The use of such multilayer hybrid junctions to produce filters covering the 40- to 110-GHz range is examined.**

## I. Introduction

THE FORMATION of a hybrid junction via a dielectric sheet or a perforated metal plate placed at 45° across the right angle intersection of two circular waveguides has been the subject of considerable investigation [1], [2]. The use of multiple dielectric layers to reduce distortion of the transmitted and reflected waves has been described by Saleh [3]. This paper will show how a three-layer dielectric can be applied to the circular-electric mode hybrid junction to yield considerably improved performance over previous designs in both unwanted mode conversion levels and broad-band equality of power division. Design techniques and measured results are presented. These results provide a better understanding of the basic loss mechanisms of the hybrid as well as a confirmation of the analytical and design techniques.

Application of such a hybrid junction to a band-splitting filter is discussed. Reduced mode conversion and uniformity of power division offer considerably improved filter performance over single-layer dielectric designs. However, as will be discussed, increasing dielectric losses near 100 GHz in presently available materials degrades the hybrid junction performance in this region.

## II. Circular Electric Mode Hybrid Junction Analysis

Fig. 1 shows the structure of a hybrid junction or directional coupler in oversize circular waveguide. While such a structure can act as a directional coupler for any propagating mode, many important applications involve use of the circular electric mode ($TE_{01}^{\circ}$) in circular waveguide. The field pattern for this mode is shown in Fig. 2.

Fig. 3(a) illustrates scattering of the $TE_{01}^{\circ}$ mode by the dielectric sheet (the field intensities are computed in Section II-A). Since the $TE_{01}^{\circ}$ mode has transverse electric field components oriented in all directions (full 360°), the complex magnitude of the transmission through and reflection from a dielectric sheet must be computed for all polarizations. Fresnel's formulas [4] give the reflection and transmission coefficients for the two primary orientations of the field ($E$ polarization has electric field parallel to plane of incidence; $H$ polarization has electric field perpendicular to plane of incidence). For the circular electric field pattern, there are four points on the circle where the field is purely $E$ polarized or purely $H$ polarized. For the electric field vector oriented at other angles, the field can

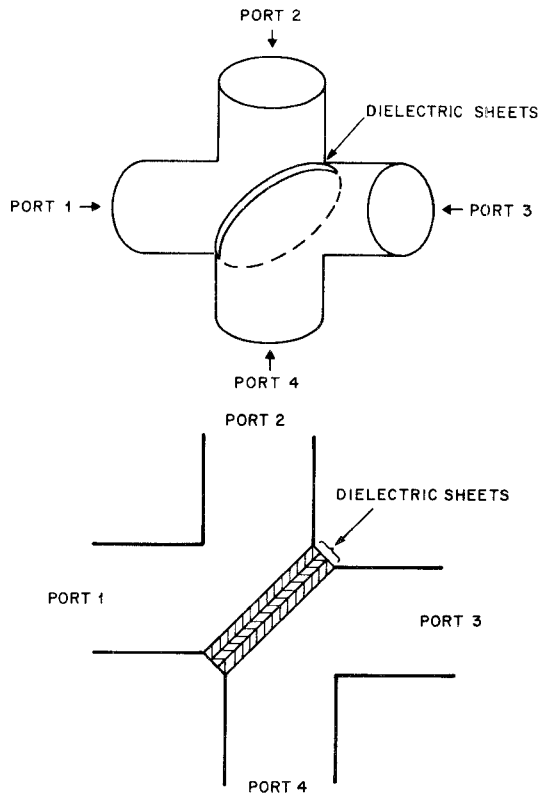


Fig. 1. Multilayer hybrid in circular waveguide.

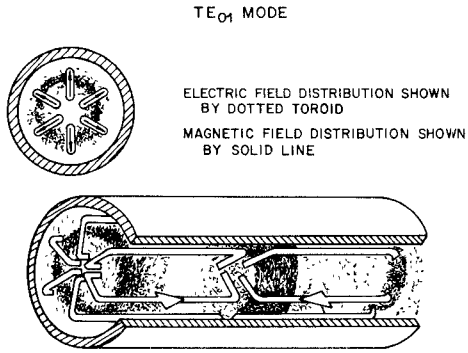


Fig. 2. Electromagnetic field configuration for the $TE_{01}^{\circ}$ mode.

Manuscript received April 23, 1979; revised August 22, 1979.
The authors are with Bell Laboratories, Holmdel, NJ 07733.

0018-9480/79/1200-0975$00.75 ©1979 IEEE

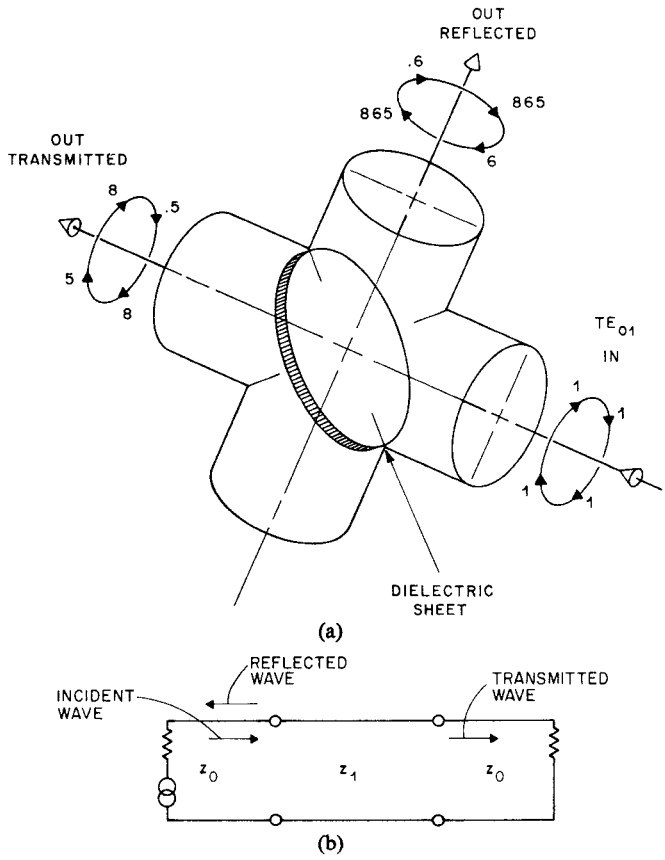


Fig. 3. $TE_{01}^{\circ}$ scattering by sheet. (a) Electric field intensity of the incident, transmitted and reflected circular electric field pattern for a dielectric sheet with $\epsilon = 7.5$, quarter-wave thick. (b) Transmission line equivalent.

always be decomposed into the $E$ and $H$ polarized components.

If the amplitudes or phases of the $E$ and $H$ polarized reflections (or transmissions) are different, then obviously the purity of the $TE_{01}^{\circ}$ mode is not maintained after reflection (or transmission) from the dielectric sheet.

In the hybrid junction there are reflections at every dielectric discontinuity with multiple reflections between interfaces. A straightforward method to calculate the total reflection (and transmission) from multiple layers is to treat it as a transmission line problem. Assuming that ray optics applied (i.e., $TE_{01}^{\circ}$ is very far from cutoff in the waveguide), the two primary polarizations may be treated as infinite plane waves impinging on the dielectric boundaries. The reflection and transmission magnitudes of any portion of the circular electric field pattern can then be computed from these two components. Previous calculations of this kind have shown good agreement with experiment [1], [2].

For each polarization, the structure of Fig. 3(a) with incident, reflected, and transmitted waves can be compared with the transmission line network of Fig. 3(b). While the reflected infinite plane wave of Fig. 3(a) comes off in a direction perpendicular to the input plane wave, and the reflected wave of Fig. 3(b) is on the same transmission line as the incident wave, the multiple reflections at the dielectric interfaces follow the same laws as the reflections at the impedance discontinuities of the transmission lines. Examination of the reflection at a dielectric interface leads to an evaluation of the characteristic impedance in the transmission-line model. From Snell's Law

$$\sin r = \frac{\sin i}{\sqrt{\epsilon}}$$

knowing $\epsilon$ (permittivity) and $i$ (angle of incidence) we can obtain $r$ (angle of refraction). Then using Fresnel's formula for the $E$ polarization the ratio of reflected to incident electric field is

$$\frac{E_1}{E_0} = \frac{\tan(i-r)}{\tan(i+r)}. \tag{1}$$

For the transmission line of Fig. 3(b) the reflection is given by

$$\frac{E_1}{E_0} = \frac{Z_1 - Z_0}{Z_1 + Z_0} = \frac{(Z_1/Z_0)-1}{(Z_1/Z_0)+1}. \tag{2}$$

The transmission line discontinuity $(Z_1/Z_0)$ in the equivalent circuit can, therefore, be obtained from Fresnel's formulas. For the $H$ polarization the equations are similar, except now the Fresnel's formula is

$$\frac{E_1}{E_0} = -\frac{\sin(i-r)}{\sin(i+r)}. \tag{3}$$

Given the means for calculating the impedance discontinuity at each dielectric or transmission line interface, scattering calculations can be performed for any number of dielectrics stacked in tandem. The reflection at and transmission through each dielectric sheet can be calculated with the assistance of the well known equation

$$\frac{Z_{IN}}{Z_0} = \frac{Z_{OUT}/Z_0 + j\tan\beta l}{1 + jZ_{OUT}/Z_0 \tan\beta l} \tag{4}$$

where $\beta l$ is the transmission phase shift through the dielectric, $Z_0$ is the characteristic impedance of the transmission line equivalent for the dielectric, $Z_{OUT}$ is the terminating impedance of the line, and $Z_{IN}$ is the equivalent impedance at the input to the dielectric sheet. Of course, the input impedance for one dielectric sheet may be the output impedance for an adjacent dielectric sheet. After calculating the input impedance for a stack of dielectric sheets, the reflection coefficient for the entire stack can be calculated from

$$\Gamma = \frac{Z_{IN} - Z_0}{Z_{IN} + Z_0}. \tag{5}$$

This must be done for two polarizations of the infinite plane wave.

### *A. Example—Single-Layer Hybrid*

An example of this analysis is presented for a single dielectric sheet with $\epsilon = 7.5$ and a thickness of 0.015 in (quarter wave at 75 GHz) placed at 45° across the junction of two circular waveguides.

The path length through the dielectric of the ray reflected from the back surface of the dielectric sheet is

given by $2(t/\cos r)$, where $t$ is the sheet thickness. However, the point at which this ray emerges from the dielectric is removed from the entrance point by a distance $2t\tan r\sin i$. The proper $\beta l$ to be used in the transmission line formula is, therefore, given by

$$\beta l = t\frac{2\pi}{\lambda_0}\left(\frac{\sqrt{\varepsilon}}{\cos r} - \tan r \sin i\right). \tag{6}$$

Application of the analyses of the previous section at 75 GHz results in the purely $H$-polarized portions of the circular-electric mode field pattern being reflected with a magnitude of 0.600 while the purely $E$-polarized portions are reflected with a magnitude of 0.867. Other portions (or polarizations) of the circular-electric field pattern will be reflected with a magnitude between these. The $TE_{01}^{\circ}$ content of the reflected field pattern is given by the average magnitude of the field around the circle. This can be obtained from the average value of the two reflection coefficients. For the example considered here the $TE_{01}^{\circ}$ reflected magnitude is

$$V_0 = \frac{1}{2}(\Gamma_H + \Gamma_E) = 0.733.$$

The magnitude of the reflected field remaining after subtracting out the $TE_{01}^{\circ}$ component is given by one-half the difference between the reflection coefficients for the $H$ and $E$ modes

$$V = \frac{1}{2}(\Gamma_H - \Gamma_E)$$
$$= 0.133.$$

Most of this remaining field exists as the $TE_{21}^{\circ}$ mode [1].

Similar calculations can be carried out for other frequencies yielding the reflected and transmitted magnitude of $TE_{01}^{\circ}$ for the above hybrid junction shown in Fig. 4. It is seen that this is a quite well balanced design to approximate a 3-dB (0.707 magnitude) hybrid junction across the 40- to 110-GHz band. The mode conversion to $TE_{21}^{\circ}$ is at about the $-17$-dB level across the whole band.

### B. Multilayer Hybrid

Several techniques for eliminating the polarization sensitivity of the transmitted and reflected wave have been suggested by Saleh [3]. In particular, a three-layer dielectric sheet has been proposed. The motivation for such a structure can be understood by considering the physics of the change in magnitude of reflection with angle of polarization. As is well known, at Brewster's angle the magnitude of reflection for the $E$ polarization becomes zero. From (1), Brewster's angle ($i$) is the angle at which $i + r = 90°$ for a particular dielectric. This is an extreme condition for which we would have very large distortion for a $TE_{01}^{\circ}$ field pattern incident upon such a dielectric sheet. By analogy, this corresponds to a match in the impedance of the transmission lines of the equivalent circuit for the $E$ polarization. The way to overcome the unequal reflection coefficients for the two sets of equivalent transmission lines (for $E$ and $H$ polarizations) is, therefore, to choose a very large dielectric constant for a center sheet such that the reflection from this single sheet for both polarizations is much larger than wanted. Then a lower dielectric constant quarter-wave matching section can be placed on each side of the center sheet to reduce the reflection coefficient to the desired value. A wide range of dielectric values can be used to adjust the reflection for either polarization to its desired value. However, Saleh [3] has pointed out that there is a unique set of dielectric constants (for a particular angle of incidence) for which the reflection coefficients can be made equal in magnitude and phase for both polarizations. This means that the reflected and transmitted circular electric field patterns are perfectly uniform around the complete circle. Applying results from Saleh [3] at 45° incidence leads to $\epsilon_1 = 1.643$ ($\epsilon_1$ = outer layer dielectric constant) and $\epsilon_2 = 15.75$ ($\epsilon_2$ = inner layer dielectric constant). Analyzing the two equivalent circuits with three transmission lines in tandem results in the magnitude of the reflected and transmitted $TE_{01}^{\circ}$ fields plotted in Fig. 5. The $TE_{21}^{\circ}$ mode-generating component is greatly reduced. There is no $TE_{21}^{\circ}$ at midband. It is at worst about 20 dB down at the band edges. While $TE_{21}^{\circ}$ has been greatly reduced, it is seen that the peak deviation from equal power to the transmitted and reflected arms is about the same as for the single-sheet hybrid previously calculated (Fig. 4).

It is apparent that the single-layer hybrid was designed to yield close to 3-dB coupling across the 40- to 110-GHz

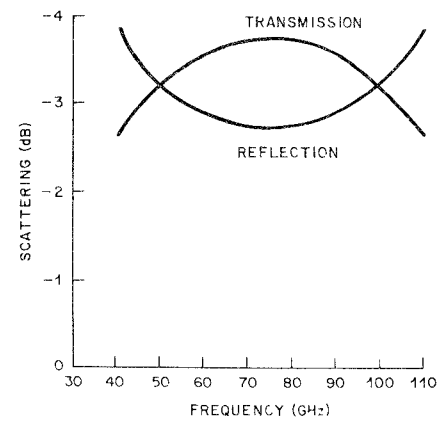


Fig. 4. Transmission and reflection for $TE_{01}$ mode single-layer dielectric hybrid.

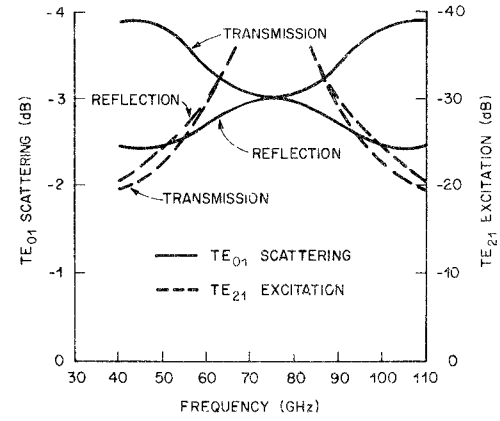


Fig. 5. $TE_{01}^{\circ}$ scattering and $TE_{21}^{\circ}$ excitation for $TE_{01}^{\circ}$ mode three-layer dielectric hybrid with zero $TE_{21}^{\circ}$ at band center.

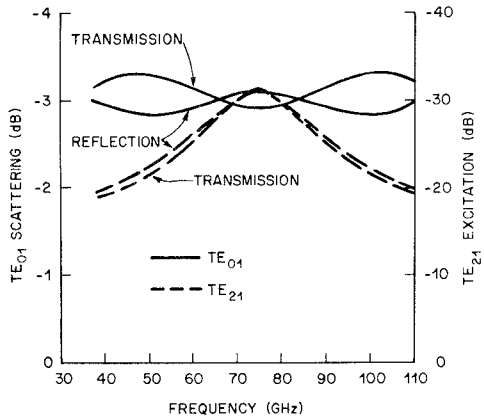


Fig. 6. $TE_{01}^{\circ}$ scattering and $TE_{21}^{\circ}$ excitation for broad-band three-layer dielectric hybrid.

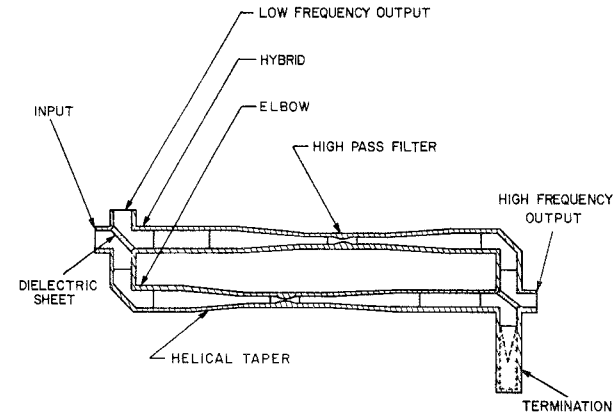


Fig. 7. Schematic cross section of circular-waveguide band diplexer.

band while the three-layer dielectric was designed to operate at the band center (75 GHz). Obviously what is needed is a design variation to produce less than an exact 3-dB power split at midband, but improve the power division at the band edges. A lower dielectric constant for both $\epsilon_1$ and $\epsilon_2$ will reduce the magnitude of the reflected $TE_{01}^{\circ}$ wave and still maintain at least some of the $TE_{21}^{\circ}$ mode reduction. Fig. 6 gives the reflected and transmitted fields for a three-layer dielectric hybrid junction with $\epsilon_1 = 1.45$ and $\epsilon_2 = 12.0$.

The equality of power split for the two output ports is now very good and while $TE_{21}^{\circ}$ excitation is down to $-31$ dB at band center it comes up to $-19$ dB at the band edges. It is still better than the single-layer dielectric hybrid for $TE_{21}^{\circ}$ excitation. The $TE_{01}^{\circ}$ uniformity of power division is also considerably better than for the single dielectric layer model. This three-layer dielectric hybrid junction has much better broad-band performance than the three-dielectric-layer hybrid junction which was optimized for midband performance.

### C. Conservation of Energy

It is instructive to sum up the nominal amount of energy contained in the $TE_{01}^{\circ}$ and $TE_{21}^{\circ}$ output waves. For the hybrid of Fig. 6 the total output energy is within one-half percent of the input energy at all frequencies. The total energy content of all other modes should, therefore, be greater than 23 dB down.

## III. Return Loss of a Band-Splitting Filter

A particularly important application of the hybrid is in a band-splitting filter (band diplexer) as shown in Fig. 7. An array of band-splitting filters is used to split the WT4 system waveguide band into seven subbands covering the 40- to 110-GHz band [5].

It is easy to show that the return loss of a band-splitting filter is obtained from

$$\text{Magnitude of } TE_{01}^{\circ} \text{ Reflected Signal} = R\left[(TE_{01}^{\circ})_T^2 - E^2(TE_{01}^{\circ})_R^2\right] \quad (7)$$

where $R$ is the reflection coefficient of the band diplexer high-pass filters (ideally, $R=1$ below cutoff and $R=0$ above cutoff), $(TE_{01}^{\circ})_R$ is the magnitude of the $TE_{01}^{\circ}$ reflected component for the hybrid, $(TE_{01}^{\circ})_T$ is the magnitude of the $TE_{01}^{\circ}$ transmitted component for the hybrid, and $E$ is the transmission coefficient for the elbow used in the band diplexer.

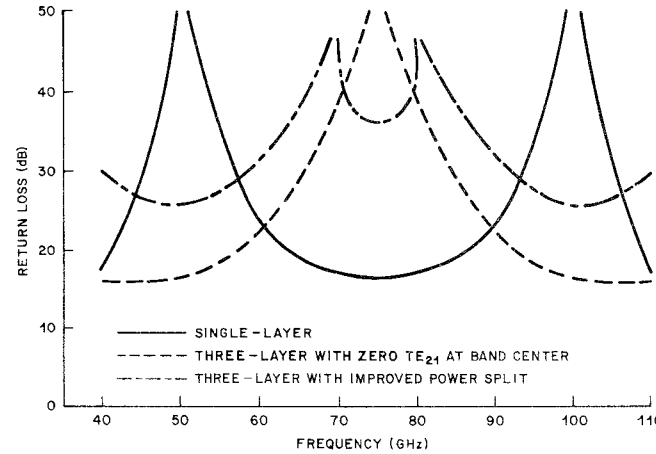


Fig. 8. Calculated return loss for band diplexers using single-layer hybrid, three-layer hybrid with zero $TE_{21}^{\circ}$ at band center, or three-layer hybrid with improved power split.

This means that if $E=1$, there will be very high return loss for a band-splitting filter when there is equal power division between the two arms of the hybrid junction ($(TE_{01}^{\circ})_R = (TE_{01}^{\circ})_T$). Using this equation and the values of $TE_{01}^{\circ}$ transmission and reflection obtained from Figs. 4–6, the plot of Fig. 8 is obtained for the return loss of band-splitting filters using the three hybrid junctions. These return loss curves apply only at frequencies below the cutoff of the high-pass filter used in the band diplexer ($R=1$).

## IV. Experimental Results

The following applies the theory presented in the previous sections to the design of actual hybrid junctions which have been fabricated and measured. Since there may be considerable variability among samples, the dielectric constants and thicknesses of the actual sheets which are being considered for use in a hybrid are determined experimentally. This is done for each sheet by measuring the $TE_{01}^{\circ}$

insertion and return losses of the sheet mounted transversely across a 2-in-diameter circular waveguide over 40 to 110 GHz. A least squares fit to the predicted insertion and return losses is then used to determine the dielectric constant and thickness. The best layers are then assembled into a hybrid junction. The performance of this hybrid is finally measured over 40 to 110 GHz. A band-splitting filter is simulated by short circuiting two of the hybrid's ports. Measurements of the simulated band-splitting filter give an indication of the performance achievable in an actual band-splitting filter.

Three sets of results shall be presented here. First, are the results for transmission and reflection of an experimental broad-band three-layer hybrid. Next, results for a simulated band-splitting filter made with this hybrid are given. Finally, data are presented for a hybrid which is not as broad band, but fabricated from dielectric material having lower dissipation loss.

### *A. Experimental Three-Layer Hybrid*

The transmission and reflection of the three-layer hybrid are given in Fig. 9. The middle layer was measured to have a dielectric constant of 13.5 and a thickness of 0.01275 in. This layer was made of magnesium titanate. The two outer layers had measured dielectric constants of 1.6 and thicknesses of 0.0416 in for one, and 0.0436 in for the other. These were foamed polystyrene pieces, machined from blocks of Eccofoam PS ($K=1.6$) obtained from Emerson and Cuming, Inc.

The measured performance curve of Fig. 9 displays the power division and mode conversion loss as discussed in Section II-B plus additional losses. The additional significant loss mechanisms contributing to the measured data of Fig. 9 are 1) the elbow-type loss occurring at the intersection of two waveguides; 2) an offset loss due to misalignment between the propagating fields and the waveguide mechanical axes; and 3) the dissipation of energy in the dielectric sheets. The elbow loss (mode conversion) is basically due to removal of the conducting sidewalls of the waveguides where they intersect and has been analyzed by Marcatili. It is given by [6]

$$\text{Loss(dB)} = -20\log\left[1-0.279\left(\frac{\lambda}{a}\right)^{3/2}\right] \qquad (8)$$

where $\lambda$ is wavelength and $a$ is the waveguide radius.

If the right angle intersection of two circular guides is cut at a 45° angle and dielectric sheets are inserted, the mechanical axes of the waveguides will be displaced due to the finite thickness of the dielectric sheets. In addition, the electromagnetic field patterns will be displaced as they are reflected or traverse the dielectric sheets. The loss (mode conversion) due to the relative offset of the mechanical and electric axes can be minimized by machining the proper amount of material from each half of the hybrid. The amount of offset loss for the hybrid of Fig. 9 has been estimated from measurements made of an empty waveguide junction offset by means of metal spacers. The dissipation loss of the sheets is obtained by

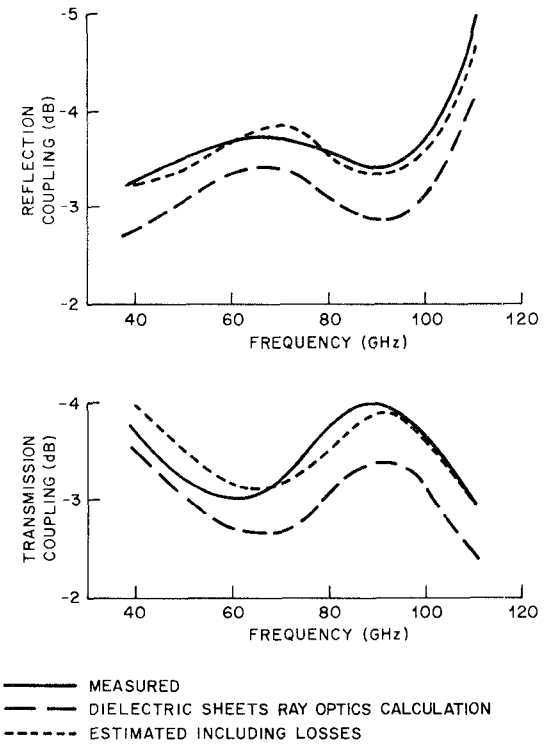


Fig. 9. Comparison of measured and calculated performance of a three-layer dielectric sheet hybrid junction.

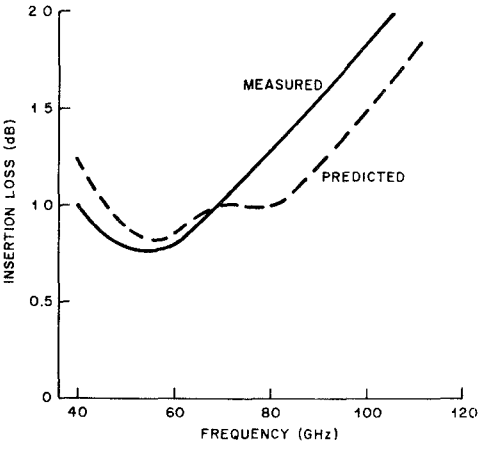


Fig. 10. Insertion loss of simulated band diplexer.

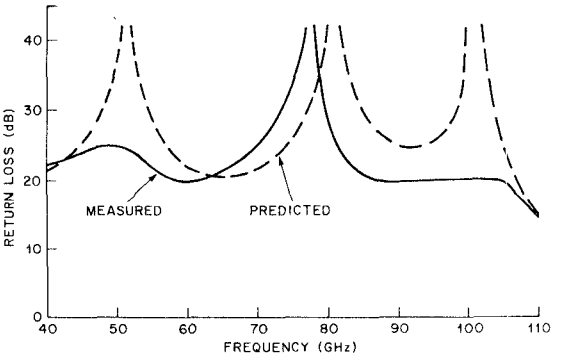


Fig. 11. Return loss of simulated band diplexer.

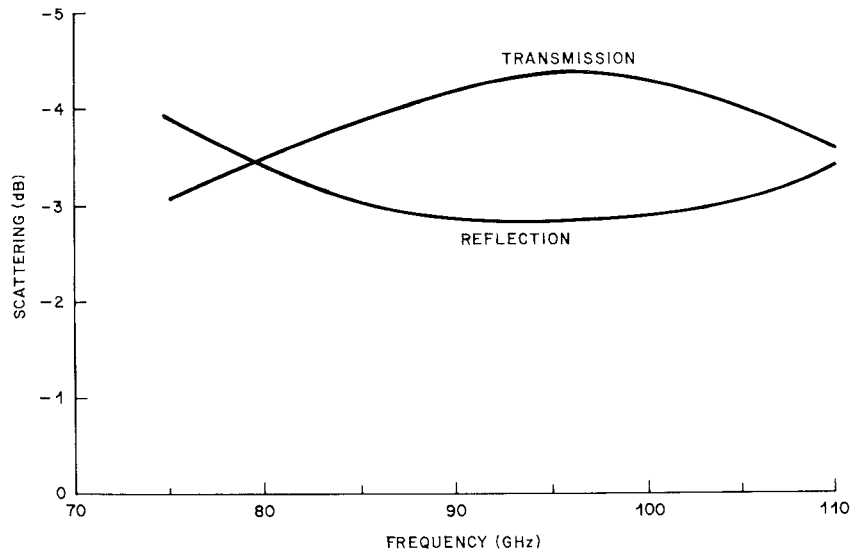


Fig. 12. Measured scattering coefficients of lowest loss hybrid.

multiplying the measured dissipation loss of the transversely mounted individual sheets by 1.414 to account for the 45° angle that the sheets make with respect to the waveguide axes. Most of the dissipation loss is in the foamed polystyrene. The Appendix provides a more detailed discussion of loss mechanisms.

### *B. Simulated Band-Splitting Filter*

A band-splitting filter can be simulated by short circuiting each of two ports of the hybrid junction. This was done for the hybrid described in the previous section.

The predicted and measured insertion and return losses are shown in Figs. 10 and 11. Metal spacers were used to locate the short-circuit planes so that optimum return loss performance was achieved over 46 to 110 GHz. The measured insertion loss varies from 1 dB at 40 GHz to 2.1 dB at 110 GHz. Improved materials are required to reduce this loss. The predicted and measured insertion losses agree to within a few tenths of a decibel. Note that the predicted 0.1-dB bump near 70 GHz was not observed in the measurements. It was probably masked by the test set, which has an accuracy of $\pm 0.1$ dB. The frequencies of the return loss minimums and maximums agree to within about 5 percent. Some of the measured maximums are smaller than predicted. This is in part due to limitations of the test set in measuring very high return losses.

The simulated band-splitting filter insertion loss is caused, in part, by imbalance in the reflection and transmission-coefficients and the mode conversion loss as derived from the transmission line model. In addition, there is the elbow-type loss of the hybrid junction, as well as loss due to the offset of the waveguide axes. The final contributor is the dissipation loss of the sheets. The insertion loss in dB is given by

$$\begin{aligned}\text{loss} = &-20\log_{10^2} + \text{transmission coefficient} \\ &+ \text{reflection coefficient} \\ &+ 2\times\text{elbow loss} \\ &+ 2\times\text{dissipation loss of sheets} \\ &+ \text{offset waveguide loss}\end{aligned}$$

or, at 110 GHz,

$$\begin{aligned}\text{loss} &= -6+2.42+4.13+2(0.08) \\ &\quad +2(0.42)+0.20 \\ &= +1.75\,\text{dB}.\end{aligned}$$

This is within about 0.3 dB of the measured value. The loss from offset can be reduced by machining off enough material from the surface of each half of the hybrid to compensate for the sheet thicknesses. This means that about 0.15 dB less loss could be achieved. In addition, if enough thicknesses were available to choose from, so that a better set of thicknesses could be used, the imbalance in the reflection and transmission of the hybrid sheets could be reduced so that 0.18 dB less loss could easily be achieved in this way. Thus it should be possible to fabricate band-splitting filters having 1.8-dB loss at 110 GHz using the materials and techniques already available and presented here.

The remaining loss components, i.e., elbow-type loss and sheet heat loss, are not as easily reduced. A more complex structure would be needed to reduce the elbow-type loss. Dielectric coatings or intentional distortions of the mirror surface may be helpful in reducing elbow loss. A reduction in dielectric material losses would be a difficult thing to achieve; commercially available materials with low enough loss are difficult to find.

### *C. Hybrid with Lower Loss Material*

A three-layer hybrid was constructed using a middle layer of magnesium titanate with a dielectric constant of 13.5 and a thickness of 0.01215 in. The outer layers were 0.0416 in thick with dielectric constants of 1.85. A foamed quartz material, Emerson and Cuming Eccofoam QR, was used for these outer layers. The main feature of this material, which was commercially available in only one dielectric constant, is its low dissipation loss. The insertion loss of a transversely mounted sheet was only a few hundredths of a decibel over 40 to 110 GHz, which is considerably less than that of the Eccofoam PS. Even though the dielectric constant of this material had a value

far from optimum for the hybrid, worthwhile information about the effects of material loss on hybrid performance were obtained using it.

The reflection and transmission of this hybrid are shown in Fig. 12 over 75 to 110 GHz. At 110 GHz, a band diplexer made using this measured hybrid would be expected to have an insertion loss of 1.6 dB. Of this, 1 dB is from hybrid imbalance, 0.2 dB is elbow-type loss in the hybrid, 0.3 dB is from material dissipation loss, and 0.1 dB is from the elbows used in the filter. For the hybrid considered alone, there is 0.5 dB measured $TE_{01}^{\circ}$ energy loss. The predicted loss is 0.2 dB from sheet mode conversion plus 0.1 dB from elbow-type loss, plus 0.17 dB from material dissipation loss, for a total of about 0.5 dB. For comparison, the measured energy loss of the hybrid considered in Section IV-A was 0.9 dB.

## IV. Conclusions

The basic methods used to design a multilayer hybrid having broad-band performance and minimal mode conversion have been presented and verified. It has been shown that use of a three-layer hybrid rather than a single-layer one in a band-splitting filter can result in lower insertion loss and improved return loss. Based upon measurements of hybrids and of a simulated band-splitting filter, the important loss mechanisms have been identified. Of these, hybrid imbalance, mode conversion at the sheets, and offset waveguide axis loss can be reduced relatively easily. However, the losses due to elbow-type mode conversion and dissipation loss in the material are more difficult to reduce.

## Appendix

### Hybrid Loss

The main contributors to the energy loss of the waveguide hybrid junction are:

1) mode conversion at the sheets;
2) elbow-type loss of open waveguide walls;
3) sheet dissipation;
4) offset of waveguide and field axes.

The first two components have already been discussed in the text. Most of the mode conversion loss at the sheets is implicitly included in the scattering coefficients computed using the lossless cascaded transmission-line model. Elbow-type loss is obtainable from Marcatili's formula [6].

Sheet dissipation and offset axes loss are determined experimentally. Sheet dissipation is obtained by measuring the $TE_{01}^{\circ}$ reflection and transmission coefficients of a sheet transversely mounted across a circular waveguide. Dissipation loss is then computable from these coefficients; the total transmitted and reflected normalized power would be unity for no dissipation loss. The loss thus determined is entirely dissipation loss since mode conversion of the normally incident $TE_{01}^{\circ}$ mode, which is far above cutoff and nearly a plane wave, is negligible. The dissipation loss of the sheet when used in a hybrid junction is then obtained by multiplying the loss of the transversely mounted sheet by 1.414 to account for the 45° angle of the ray path.

Due to the finite thickness of the sheets used in the hybrid, the axes of the electromagnetic field and the output waveguide are offset with respect to each other. This will cause additional loss. The offset axes loss used in obtaining predicted overall hybrid performance is obtained by measuring the transmission of the $TE_{01}^{\circ}$ mode across a hybrid junction having spacers but no sheets present. The loss, after subtracting the elbow-type loss from Marcatili's formula, is that due to the difference in offset between the field and waveguide axes for an empty hybrid. The dielectric sheets will tend to compensate the amount of offset because of ray bending at the dielectric interfaces. The offset loss used in the computation includes this compensation effect.

The predicted loss of the broad-band three-layer hybrid described in the text shall be computed at 110 GHz as an example.

The computed $TE_{01}^{\circ}$ reflection and transmission coefficients of the hybrid are $-4.13$ and $-2.42$ dB, respectively. These are computed using the cascaded dissipationless transmission-line model. The center sheet has a dielectric constant of 13.5 and is 0.01275 in thick. The outer sheets have dielectric constants of 1.6 and thicknesses of 0.0416 and 0.0436 in, respectively.

The mode conversion loss in the hybrid due to distortion of the $TE_{01}^{\circ}$ mode by the sheets is, therefore

$$-10\log_{10}(10^{-(4.13/10)}+10^{-(2.42/10)})=0.18\,\text{dB}.$$

This loss is implicitly included in the computed scattering coefficients.

Elbow-type loss is computed from (8). For a 2-in-diameter circular-waveguide elbow at 110 GHz, the elbow-type loss which should be included in each scattering coefficient amounts to 0.08 dB.

Sheet dissipation loss was measured as 0.15 dB in each outer sheet, when transversely mounted in the waveguide. The dissipation in the center sheet was negligible. Hybrid sheet dissipation loss is, therefore, predicted to be $1.414\times(0.15+0.15)=0.42$ dB.

The loss across an empty hybrid was measured to be 0.3 dB. The offset waveguide loss is therefore 0.3 dB minus 0.08 dB elbow-type loss, or 0.2 dB. It is estimated that ray bending at the sheet interface reduces this loss to 0.1 dB.

Summing the losses yields the following scattering coefficients:

$$\text{reflection} = -4.13-0.08-0.42-0.1=-4.7\ \text{dB}$$
$$\text{transmission} = -2.42-0.08-0.42-0.1=-3.0\ \text{dB}.$$

The measured reflection and transmission coefficients were $-5.0$ and $-3.0$ dB, respectively (Fig. 9).

## Acknowledgment

The authors wish to thank A. C. Chipaloski and B. T. Verstegen for performing much of the experimental work, and S. H. Cureton and C. D. Nowack for assistance in preparing the figures.

## References

[1] S. Iiguchi, "Michelson interferometer type hybrid for circular $TE_{01}$ wave and its application to band-splitting filter," *Rev. Elec. Commun. Lab.*, vol. 10, pp. 631–642, 1962.
[2] E. A. Marcatili and D. L. Bisbee, "Band-splitting filter," *Bell Syst.*

*Tech. J.*, vol. 40, pp. 197–212, 1961.
[3] A. A. M. Saleh, "Polarization-independent, multilayer dielectrics at oblique incidence," *Bell Syst. Tech. J.*, vol. 54, pp. 1027–1049, 1975.
[4] M. Born and E. Wolf, *Principles of Optics.* London, England: Pergamon, 1970, pp. 38–41.
[5] E. T. Harkless *et al.*, "WT4 millimeter waveguide system: Channelization," *Bell Syst. Tech. J.*, vol. 56, pp. 2089–2101, 1977.
[6] E. A. Marcatili, "Miter elbow for circular electric mode," in *Proc. Symp. on Quasi-Optics*, Brooklyn, NY: Polytechnic Press, 1964, pp. 535–543.

# Cylindrical $TE_{011}/TM_{111}$ Mode Control by Cavity Shaping

HERBERT L. THAL, JR. MEMBER, IEEE

***Abstract*—An appropriate modification of the shape of a cylindrical filter cavity has been used to separate the degenerate $TM_{111}$ (doublet) modes while at the same time providing a slight increase in the already high unloaded $Q$ of the desired $TE_{011}$ mode. Experimental results of mode frequencies and unloaded $Q$'s are tabulated for a family of shaped cavities. Two low-loss filters utilizing these cavities are discussed. The general correspondence between modes of spherical, cylindrical and rectangular cavities and waveguides is described in order to place the performance of intermediate shapes in perspective.**

## I. Introduction

THE $TE_{011}$ cylindrical cavity mode is potentially attractive for use in low-loss filters [1], [2] since it offers a higher unloaded $Q$ than other modes having comparable cavity volumes, and it is easily tuned by a noncontacting, movable end wall. However, it is degenerate with a pair of $TM_{111}$ modes which must be perturbed in some manner to make the $TE_{011}$ mode usable. The required perturbation increases as the bandwidth of the filter increases; for multiplexer applications it is necessary to have the output cavity (at least) free of spurious modes over the entire multiplexed bandwidth since a weakly coupled resonance could introduce an absorption notch in one of the other channels even without producing a spurious transmission response. Previously described reactive or dissipative techniques degrade the $TE_{011}$ $Q$ in the process of controlling the $TM_{111}$ mode whereas the approach covered in this paper yields a significant detuning of the $TM_{111}$ resonance with a small increase in the $TE_{011}$ $Q$ as a by-product.

## II. $TM_{111}$ Mode Control

This method may be understood by relating the modes of a cylindrical cavity to those of a spherical cavity [3] as illustrated in Fig. 1. (General mode relationships are given in the Appendix.) The normalized parameter $Q\delta/\lambda_0$ is shown for each mode; $\delta$ is the skin depth and $\lambda_0$ is its resonant wavelength. The value of 0.641 for the $TE_{011}$ mode is close to the maximum of 0.659 which occurs at a $D/L$ of 1.00. Because of its symmetry the sphere has fewer different resonant frequencies but higher order degeneracies at each as indicated by the superscripts in parentheses. In general the spherical mode $Q$'s are higher than the corresponding cylindrical ones. If the cavity were deformed from a cylindrical to a spherical shape, the resonances would move continuously from one family to the other as indicated schematically by the straight lines. Thus the figure suggests that there should be intermediate shapes which isolate the desired (cylindrical) $TE_{011}$ mode from the degeneracies that exist in the cylindrical and spherical cases.

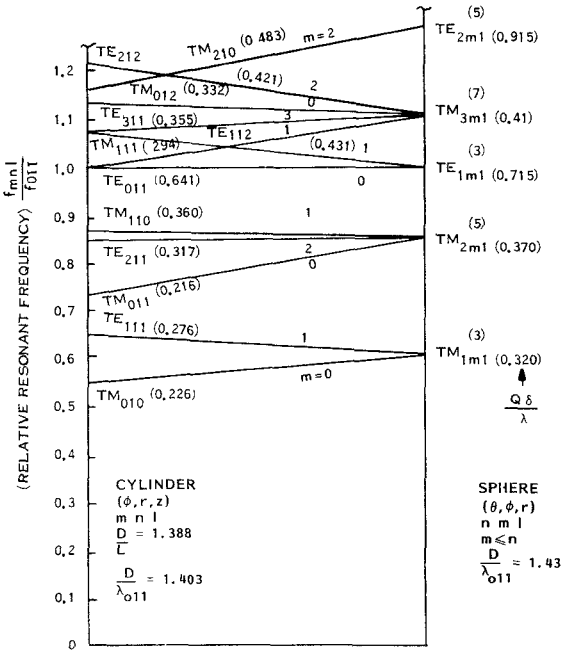


Fig. 1. Resonances of cylindrical and spherical cavities.

A cavity with chamfered ends as shown in Fig. 2 provides a mechanically convenient transitional shape which has been studied experimentally. Measurements

Manuscript received April 17, 1979; revised August 17, 1979.
The author is with Space Division, General Electric Company, Philadelphia, PA 19101.

0018-9480/79/1200-0982$00.75 ©1979 IEEE